

FRACTURE OF LIGHTLY REINFORCED CONCRETE BEAMS: THEORY AND EXPERIMENTS

J. Planas, G. Ruiz, and M. Elices,
Departamento de Ciencia de Materiales. ETS de Ingenieros de Caminos,
Canales y Puertos. Universidad Politécnica de Madrid. Madrid, Spain

Abstract

This contribution presents some recent results of an experimental program aimed at revealing the basic aspects of fracture behavior of lightly reinforced concrete beams. Micro-concrete beams of various sizes, with various steel ratios and various bond properties of the reinforcing bars have been tested. Special care was exerted to achieve low scatter and to produce an exhaustive material characterization. This included the determination of fracture properties, steel stress-strain curve and bond-slip properties. The experimental results are discussed, based on a numerical simulation that includes the cohesive crack behavior of concrete and the bond-slip of the reinforcement. The results show good agreement between the theoretical and experimental curves.

1 Introduction

Lightly reinforced beams can fail in a brittle manner upon overloading. The usual code provisions give a lower bound for the reinforcement devised, in principle, to prevent the brittle behavior. However, most codes do not take into account that this kind of failure is dominated by fracture mechanics, thus giving rise to a size effect. The interest of the subject, and its apparent simplicity, made it one of the main objects of study within ESIS Committee 9, and promoted various experimental researches

(Bosco, Carpinteri and Debernardi 1990ab; Baluch, Azad and Ashmawi 1990; Hededal and Kroon 1991) and quite a few theoretical analyses, based either on linear elastic fracture mechanics (Bosco and Carpinteri 1990, 1992; Baluch, Azad and Ashmawi 1990; Massabò 1994), or on cohesive crack concepts (Hawkins and Hjørsetet 1990, Hededal and Kroon 1991, Gerstle et al. 1992; Ulfkjær et al. 1994; Ruiz, Planas and Elices 1993; Ruiz and Planas 1994).

Among the foregoing references, only the works of Hededal and Kroon (1991) and of Ruiz and Planas (1994) take into account the possibility of bond-slip between reinforcing bars and concrete. However, both the experiments of Hededal and Kroon (1991) and the theoretical analysis showed that bond-slip influences substantially the response of the beams. On the other hand, the available experiments did not provide *independent* measurement of all the properties of the materials relevant to the analysis, particularly of the bond-slip properties. Thus, the need was felt for an experimental research covering the determination of all the properties of concrete, steel and steel-concrete interface, as well as the tests of lightly reinforced beams of various sizes, with various reinforcement ratios and adherences. This paper gives an outline of some of the most relevant results of the research.

A very brief outline of the theoretical approximation is given in Section 2. The materials and specimens are described in section 3. Section 4 summarizes the experimental procedures. The experimental results are presented and discussed in section 5.

2 Theoretical outline

As previously pointed out, two general approaches have been used to analyze the experimental results. The first approximation uses LEFM to analyze fracture, with the action of reinforcement represented by a pair of concentrated load lines on the crack faces (Bosco and Carpinteri 1990, 1992; Baluch, Azad and Ashmawi 1990; Massabò 1994). This approach describes reasonably well the observed load-deflection behavior once the crack tip overcomes the reinforcement, but cannot describe the initial stages of cracking because of the limitations inherent in LEFM.

The second general approach considers that the main crack developing at the central cross section can be modeled as a cohesive crack (Hawkins and Hjørsetet 1990, Hededal and Kroon 1991, Gerstle et al. 1992; Ulfkjær et al. 1994; Ruiz, Planas and Elices 1993; Ruiz and Planas 1994). However, various secondary hypotheses and computational strategies are used by the various authors. In most cases, adherence between steel and concrete is considered as perfect (Hawkins and Hjørsetet 1990; simplified model in Hededal and Kroon 1991; Gerstle et al. 1992; Ulfkjær et al. 1994; Ruiz, Planas and Elices 1993).

The numerical model of Hededal and Kroon (1991) is the first to take into account the bond-slip, in a manner very similar to that chosen by Ruiz and Planas (1994) and in this work. The basic idea is to assume a

constant shear stress at the interface of the reinforcing bars (rebars) and the concrete, as in the classical paper of Bazant and Cedolin (1980). From the equilibrium condition, the slip length can be easily related to the pull-out stress (or force) and from the stress-strain curve of the rebar the protrusion of the bar out of the concrete can be easily found. If the bar is assumed to be elastic-perfectly plastic, the results are those shown in Fig. 1a. This is the underlying approximation in both the work of Hededal and Kroon (1991) and in that of the authors. The difference in their approaches lies in how the action of steel on concrete is implemented.

Hededal and Kroon (1991) simplify the problem by putting the resultant of the actions (force on the bar) as a pair of concentrated loads on the faces of the crack (Fig. 1b). Since the preliminary analyses using perfect adherence (Ruiz, Planas and Elices 1993) showed that when the reinforcement action is lumped on the crack faces, the results are sensitive to the size of the zone over which the rebar force is assumed to be distributed (and, indirectly, the results are sensitive to the size of the elements used in the numerical analysis!). To overcome this difficulty, Ruiz and Planas (1994) used the approximation shown in Fig. 1c, in which the resultant force of the steel on the concrete is applied at the centroid of the shear stress distribution. In the present work, the full stress distribution is taken into account (Fig. 1d).

A numerical method consisting in an enhanced version of Petersson's (1981) influence method (Planas and Elices 1991) was used. The actions of the steel on the concrete were introduced as internal stresses by computing the normal stresses generated by the loadings in Fig. 1c-d on an uncracked specimen, much in the way shrinkage is treated in previous works (Planas and Elices 1992, 1993). To compute this internal stress distribution, an analytical approximation is used based on Melan's (1932) elastic solution for a line load inside of a half space; to correct for the finite depth of the specimen, a linear stress distribution is superimposed on Melan's solution so as to satisfy equilibrium of forces and moments (see Ruiz and Planas 1994 for details).

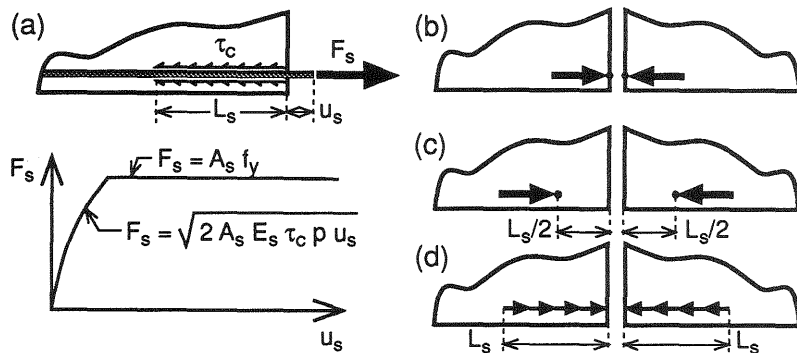


Fig. 1. Simplified descriptions of bond-slip (a) and action of steel on concrete (b-d)

The case in Fig. 1d requires integration of Melan's equation; analytic integration was performed with the help of a computer mathematical package. This analytical approach was chosen because in this way the situation of the reinforcement is not constrained by the underlying finite element grid, and any cover can be used.

Although at present the model implements elastic-perfectly plastic behavior for steel and rigid- perfectly plastic response for bond-slip, any stress-strain curve could be assumed for steel and, similarly, any shear stress-slip curve can be included for the bond-slip behavior.

The equations governing the model show that four non dimensional parameters govern all the response when beams of the same span-to-depth and relative cover are considered. The basic material properties are the elastic moduli of concrete, E_c , and steel, E_s , the tensile strength of concrete f_t , the fracture energy of concrete G_F , the yield stress of steel f_y and the bond shear strength τ_c . These combine with the geometrical properties to give the governing parameters:

$$D^* = \frac{D}{l_{ch}} , \quad \rho = \frac{A_s}{A_c} , \quad f_y^* = \frac{f_y}{f_t} , \quad \beta = \frac{\tau_c E_c p l_{ch}}{f_t E_s A_s} \quad (1)$$

where D is the beam depth, l_{ch} is the concrete characteristic size $l_{ch} = E_c G_F / f_t^2$; ρ is the reinforcement ratio, A_s the steel cross-section and A_c the beam cross-section; p is the perimeter of the rebars. Obviously, β is the parameter characterizing the bond-slip behavior. Its value is infinity for perfect bond, and zero for bars loose in a hole along the concrete.

Bosco and Carpinteri (1990) proposed to characterize the response of the beam by a non dimensional brittleness number N_p . This brittleness number is written in terms of the foregoing parameters as

$$N_p = \rho f_y^* \sqrt{D^*} \quad (2)$$

when Irwin's relationship $K_{IC} = \sqrt{E_c G_F}$ is assumed between the toughness and the fracture energy (which must be valid if LEFM applies, as assumed by Bosco and Carpinteri).

3 Materials and specimens

3.1 Micro-concrete

A single micro concrete mix was used throughout the experimentation, made with a siliceous aggregate with 5 mm maximum size and rapid hardening Portland cement (ASTM type III). The mix proportions were 0.45:1.95:0.6:0.5:1 (coarse sand:medium sand:fine sand:water:cement) with a cement contents of 500 kg/m³. All the specimens were cast in steel molds and then wrap-cured for 24 hours, then demolded and stored in a moist chamber for three weeks and then under water until testing time (8 weeks). Table 1 shows the characteristic parameters of the micro-concrete determined in the various characterization tests.

Table 1. Micro-concrete characteristics

	slump mm	age weeks	$f_c^{(a)}$ MPa	$E_c^{(a)}$ GPa	$f_{ts}^{(b)}$ MPa	$E_c^{(c)}$ GPa	G_F N/m	l_{ch} mm
mean	120	8	39.5	30.5	3.8	30.2	62.5	130
std. dev.	12	—	1.6	2.0	0.34	2.6	4.7	—

(a) Cylindrical specimens, compression. (b) Cylinder splitting (Brazilian).
(c) From initial CMOD compliance of notched beams.

3.2 Steel

Standard rebars are too large for the beam sizes considered in this experimental program. Therefore, commercial wires with a nominal diameter of 2.5 mm were used. The wires were originally smooth, so that to achieve a higher adherence, v-shaped ribs we stamped on them at a 2 mm spacing (Fig. 2a). The reduction in diameter at the deepest point of the ribs was 7.5%, while 10% protrusions appeared on both sides of the rib. Table 2 shows the elastic modulus E_s , the ultimate strength σ_u , the 0.2% offset yield strength $\sigma_{0.2}$, and the ultimate strain, ϵ_r , for both smooth and ribbed wires. Nominal values of the diameter were used to determine the parameters shown in the table. Fig. 2b shows the stress-strain curves of the two types of wire.

3.3 Characterization and control specimens

Cylindrical specimens 150 mm in length and 75 mm diameter were cast, 12 for compression tests and 12 for splitting tests. Pull-out specimens consisting in prisms 75×75×150 mm with a wire embedded along its longitudinal axis were also cast, 10 for each kind of wire, smooth or ribbed.

Table 2. Properties of the reinforcement steel bars

Wire type	E_s (GPa)	σ_u (MPa)	$\sigma_{0.2}$ (MPa)	ϵ_r (%)
smooth	200 ± 4	608 ± 5	568 ± 6	3.5
ribbed	162 ± 8	587 ± 16	538 ± 21	2.3

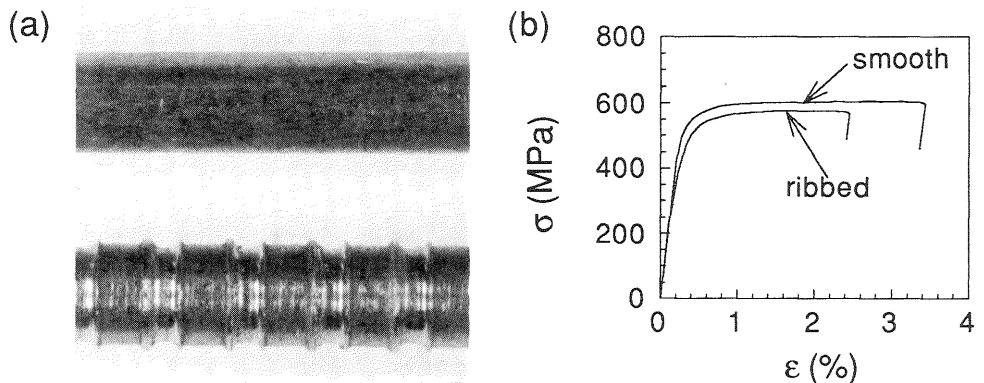


Fig. 2. Smooth and ribbed wires (a) and their stress-strain curves (b)

Plain concrete beams were used to characterize concrete fracture properties. All the beams were 50 mm in thickness and their length was 4.5 times their depth; 24 beams were 75 mm in depth, 4 beams 150 mm, and 2 beams 300 mm. Notches were sawn before testing at the central cross-section with a depth of half the total beam depth ($a_0/D = 0.5$)

3.4 Reinforced micro-concrete specimens

Table 3 and Fig. 3 summarize the dimensions and reinforcement ratio of the reinforced concrete beams. The specimens were cast in metallic molds, with the reinforcing wires protruding at the ends through holes in the mold walls. The micro concrete was compacted on a vibrating table. During casting and vibration the wires were tensioned by nuts in order to hold them in place. Just after the end of the manipulation, the tension of the wires was released. After demolding, the wires were left protruding from the end of the beam, as sketched in Fig. 3. No hooks or anchors were used.

4 Experimental procedures

4.1 Characterization and control tests

Compression and Brazilian tests were carried out on the cylindrical specimens according to ASTM C-39 and C-469, and ASTM C-496 (except for a reduction in size). Stable three-point bend tests on notched beams were carried out to determine the fracture properties of concrete following the procedures devised by Elices, Guinea and Planas (1992). The tests were performed in CMOD control, at a constant rate proportional to the beam depth [rate($\mu\text{m}/\text{min}$) = 0.0667 D(mm) for first 25 min, followed by rate($\mu\text{m}/\text{min}$) = 0.333 D(mm) to end of test].

Table 3. Reinforced beam characteristics

Characteristics	Specimen Denomination ^(a)						
	D1-1X	D1-2X	D2-1X	D2-2X	D2-4X	D3-2X	D3-4X
D (mm)	75	75	150	150	150	300	300
number of wires	1	2	1	2	4	2	4
steel ratio, ρ (%)	0.130	0.260	0.065	0.130	0.260	0.065	0.130
No. specimens ^(b)	8+8	2+2	4+4	4+4	2+2	2+2	2+2

(a) 'X' is a place holder for 'S' = smooth wire, or 'R' = ribbed wire.

(b) Half with smooth wire + half with ribbed wire.

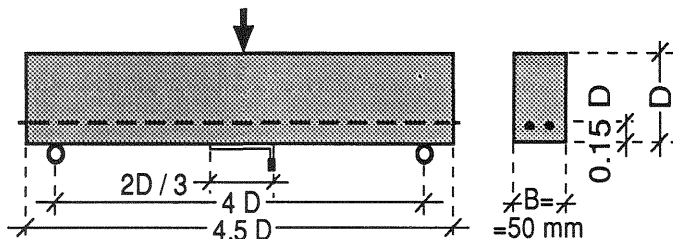


Fig. 3. Beam dimensions

Pull-out tests were carried out by pulling the wire at a constant displacement rate while keeping the concrete surface compressed against a steel plate. The load and the relative displacements between the wire and the concrete surfaces at both ends of the specimen were measured and recorded.

4.2 Reinforced beams tests

The reinforced beams were tested in three-point bending as sketched in Fig. 3. The test was controlled by means of an extensometer centered on the tensioned face of the beam (Fig. 3) which was driven at a fixed rate proportional to the beam depth [rate($\mu\text{m}/\text{min}$) = 0.0267 D(mm) during the first 20 min of the test, and rate($\mu\text{m}/\text{min}$) = 0.133 D(mm) up to complete failure].

5 Results and discussion

The main results for standard tests are included in Tables 1 and 2 and in Fig. 2b. The pull-out and reinforced beam tests results are described in the following paragraphs.

5.1 Pull-out tests

Fig. 4 shows the load-slip curves for two typical pull-out tests (full lines). Also shown are the theoretical curves corresponding to the simplified model of Fig. 1a. For the smooth wires, that slipped before breaking, τ_c was calculated as the peak force divided by the contact area. For the ribbed bars, that broke before full slip, τ_c was determined by fitting the expression in Fig. 1.a to the F-u curve. In both cases an initial s-shaped portion appeared due to accommodation of the test device; this part has been eliminated in the theoretical fit as shown in the figure. The agreement between the experimental curves and the simple theory is good for the ribbed wire, and only acceptable for the smooth one.

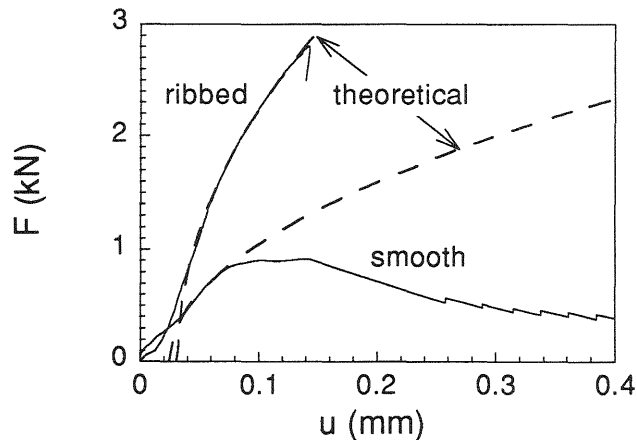


Fig. 4. Pull-out test results for smooth and ribbed wires

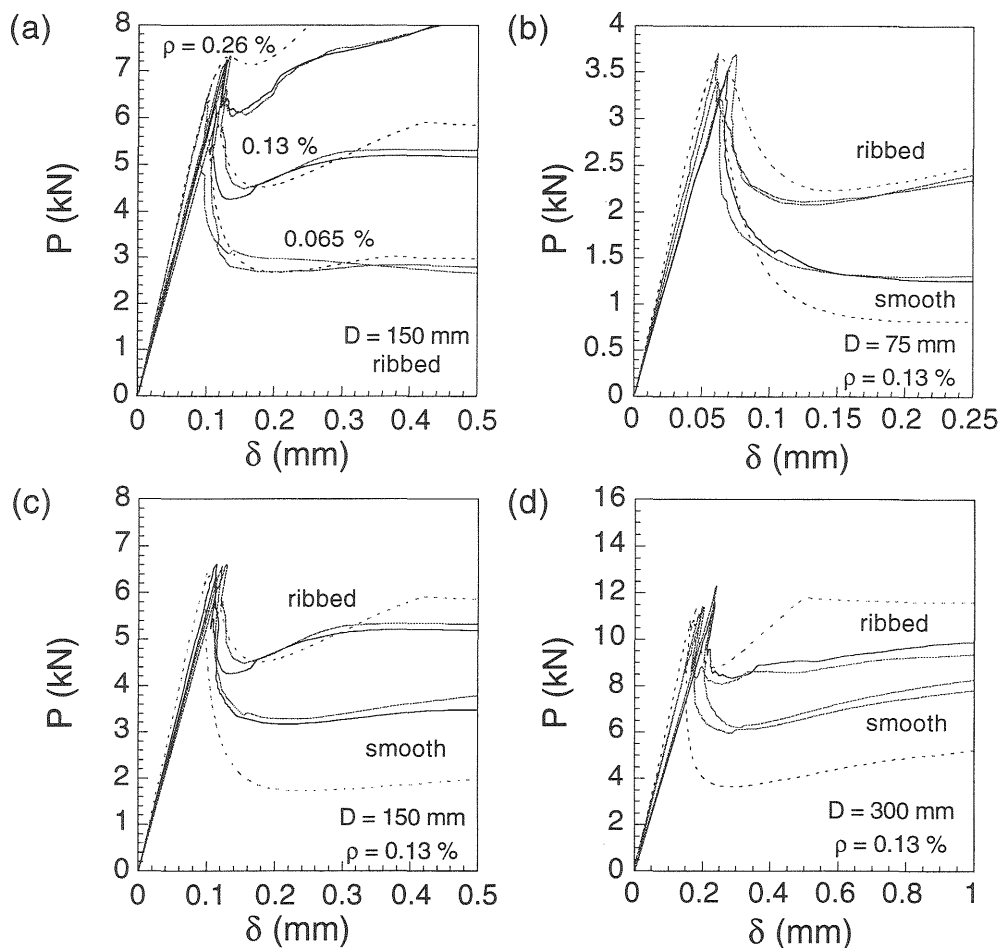


Fig. 5. Experimental (full lines) and numerical (dashed lines) P- δ curves. (a) Influence of the reinforcement ratio. (b-d) Influence of the bond strength on beams with the same reinforcing ratio but different depth ($D = 75, 150$ and 300 mm)

The values of τ_c deduced from these tests were 0.52 ± 0.19 MPa for smooth wires and 5.3 ± 1.8 MPa for ribbed wires. In both cases the scatter (standard deviation) is over 30%; this, on the one hand, quite reduces the predictive ability of the model, and, on the other hand, indicates that further refinements of the model may be meaningless: the extra accuracy would be completely blurred by the larger scatter of the bond-slip strength.

5.2 Reinforced beams tests

Fig. 5a-d show some of the experimental load-displacement curves for the reinforced beams (full lines) compared to numerical predictions (dashed lines). The theoretical predictions were produced using the material constants derived from the characterization tests. For the steel, an elastic-perfectly plastic model is used with E and f_y equal to the experi-

mental values in Table 2 (f_y is identified with the ultimate tensile strength σ_u). For the concrete, a quasi-exponential softening has been used with a critical crack opening $w_c = 5 G_F/f_t$ (for details on this curve, see Planas and Elices 1991). The value of f_t was approximated by the cylinder splitting strength in Table 1, and the values of E and G_F are those in that Table too. The values of the bond strength used in the computations were those obtained in the pull-out tests (see §5.1).

Fig. 5a shows the influence of steel ratio on the $P-\delta$ curves of 150 mm depth beams, reinforced with ribbed bars. Figs. 5b-d compare the $P-\delta$ curves for beams reinforced with ribbed and smooth wires (for identical steel ratios but different depths). The numerical predictions are reasonably good if one takes into account that the model includes strong simplifications, that the parameters have been determined in independent tests and that a large scatter was present in the pull-out tests. Better fits could be obtained by fine tuning the softening curve, the stress-strain curve of steel, and the bond-slip relationship.

Acknowledgments. The authors gratefully acknowledge financial support for this research provided by DGICYT and CICYT, Spain, under grants PB93-0031 and MAT 94-0120-C03. They also thank Prof. Fernández Cánovas for the facilities given to make the specimens in his Laboratory, and Cementos Portland S. A. for supplying the cement.

6 References

- Baluch, M. H., Azad, A. K. and Ashmawi, W. (1990) Fracture mechanics application to reinforced concrete members in flexure, in **Applications of Fracture Mechanics to Reinforced Concrete** (ed. A. Carpinteri) Elsevier Applied Science, London, 413-436.
- Bazant, Z. P., and Cedolin, L. (1980) Fracture mechanics of reinforced concrete. **J. of the Eng. Mech. Div. (ASCE)** 106, 1257-1306.
- Bosco, C. and Carpinteri, A. (1990) Fracture mechanics evaluation of minimum reinforcement in concrete structures, in **Applications of Fracture Mechanics to Reinforced Concrete** (ed. A. Carpinteri) Elsevier Applied Science, London, 347-377.
- Bosco, C. and Carpinteri, A. (1992) Fracture behavior of beam cracked across reinforcement. **Theor. Appl. Fract. Mech.**, 17, 61-68.
- Bosco, C., Carpinteri, A., and Debernardi, P.G. (1990a) Fracture of reinforced concrete: Scale effect and snap-back instability. **Engineering Fracture Mechanics**, 35(4-5), 665-667.
- Bosco, C., Carpinteri, A., and Debernardi, P.G. (1990b) Minimum reinforcement in high-strength concrete. **Journal of Structural Engineering (ASCE)**, 116(2), 427-437.

- Elices, M., Guinea, G. V., and Planas, J. (1992) Measurement of the Fracture Energy using Three Point Bend Tests. 3. Influence of cutting the P- δ tail. **Materials and Structures**, 25, 327-334.
- Gerstle, W. H., Dey, P. P., Prasad, N. N. V., Rahulkumar, P. and Xie, M. (1992) Crack growth in flexural members—A fracture mechanics approach. **ACI Structural Journal**, 89(6), 617-625.
- Hawkins, N. M. and Hjørsetet, K. (1990) Minimum reinforcement requirements for concrete flexural members, in **Applications of Fracture Mechanics to Reinforced Concrete** (ed. A. Carpinteri) Elsevier Applied Science, London, 379-412.
- Hededal, O. and Kroon, I.B. (1991) Lightly reinforced high-strength concrete. M. SC. Thesis. Ålborg University, Denmark.
- Massabò, R. (1994) Meccanismi di rottura nei materiali fibrorinforzati. PhD Thesis. Ingegneria Strutturale. Politecnico di Torino, Italy.
- Melan, E. (1932) Der Spannungszustand der durch eine Einzelkraft im Innern beanspruchten Halbschiebe. 2 . **Angew. Math. Mech.**, 12.
- Petersson, P. E. (1981) Crack growth and development of fracture zone in plain concrete and similar materials. Report TVBM-1006. Lund Institute of Technology. Sweden.
- Planas, J. and Elices, M. (1991) Nonlinear fracture of cohesive materials. **International Journal of Fracture**, 51, 139-157.
- Planas, J. and Elices, M. (1992) Shrinkage eigenstresses and structural size-effect, in **Fracture Mechanics of Concrete Structures** (ed Z.P. Bazant) Elsevier Applied Science, London, 939-950.
- Planas, J. and Elices, M., (1993) Drying shrinkage effect on the modulus of rupture, in **Creep and Shrinkage of Concrete**, (eds Z.P. Bazant and I. Carol) E & FN Spon, London, 357–368.
- Ruiz, G. and Planas, J. (1994) Propagación de una fisura cohesiva en vigas de hormigón débilmente armadas: modelo de la longitud efectiva de anclaje. **Anales de Mecánica de la Fractura**, 11, 506-513.
- Ruiz, G., Planas, J. and Elices, M. (1993) Propagación de una fisura cohesiva en vigas de hormigón débilmente armadas. **Anales de Mecánica de la Fractura**, 10, 141-146.
- Ulfkjær, J.P., Hededal, O., Kroon, I. and Brincker, R. (1994) Simple application of fictitious crack model in reinforced concrete beams—Analysis and experiments, in **Size Effect in Concrete Structures** (eds. H. Mihashi, H. Okamura and Z.P. Bazant), E & F.N. Spon, London, 281-292.

APPLICATIONS OF LINEAR ELASTIC FRACTURE MECHANICS TO REINFORCED AND PRESTRESSED CONCRETE STRUCTURES

L. Goffi
Department of Structural Engineering,
Politecnico di Torino, Italy

Abstract

Starting from previous studies, the report deals with the application of Linear Elastic Fracture Mechanics to reinforced and prestressed concrete structures. A particular correlation is established between the critical bending moments of a beam in plain, reinforced and prestressed concrete. For these last structures, are considered both the cases of unbonded and bonded reinforcement.

1 Introduction

The author had published a paper on the application of Fracture Mechanics to reinforced concrete structures submitted to bending moments, in the hypothesis of High Strength Concrete (HSC) -C70/80, whose high brittleness makes it suitable to be treated, at least in first approximation, within LEFM.

Starting from the papers quoted in bibliography (Okamura, Watanabe, Carpinteri and others), we consider a rectangular cross section ($b \times d$ see